Chapter VII

Adsorption using Treated Gallus gallus domesticus beaks (TGGDB)

Chapter VII

Adsorption using Treated *Gallus gallus domesticus* Beaks (TGGDB)

Employment of treated *Gallus gallus domesticus* beads (TGGDB) as an adsorbent for the selected anions is discussed in this chapter.

7.1 Microscopic Analysis

More granular particles are obvious in figure 7.1 b, microscopically representing TGGDB against its raw counterpart (fig 7.1a).

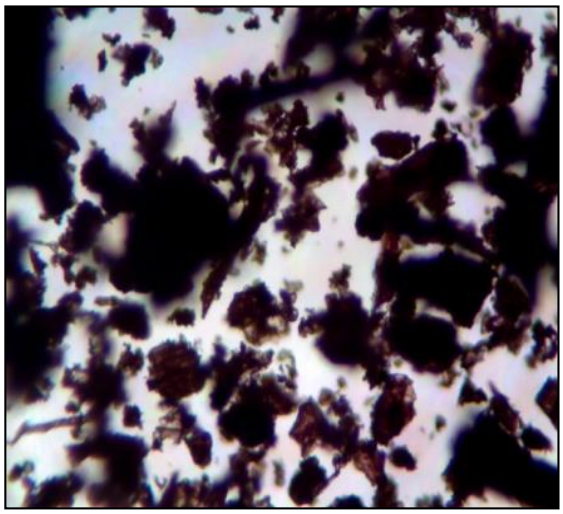

Figure 7.1 a Raw GGDB

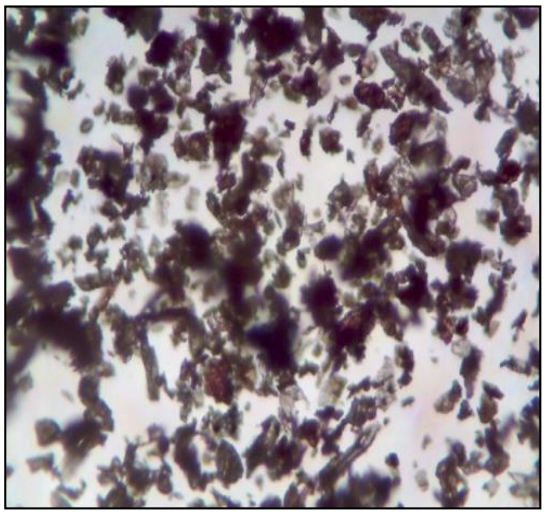

Figure 7.1b Treated GGDB

7.2 Physio- Chemical Characteristics

Notable values for the parameters bulk density, specific gravity, ash/moisture contents, water/acid soluble nature are evident for TGGDB of 0.18 mm particle size as listed in Table 7.1. This shows an appreciable characteristic of the material in the in the process of removing inorganic contaminants, thus leading to prevention of suspension[1]. Presence of surface acidic groups/ higher carbon content furnishes greater number of active sites. The mesoporous texture of TGGDB is supported by the total surface area (30.24 m^2/g) and mean pore volume (3.5 nm) parameters as observed from BET/ BJH.[2]

Table 7.1 Physio- Chemical Characteristics

Properties	TGGDB (0.18 mm)
pH	6.36
Conductivity (mV)	30.33
Moisture (%)	1.12
Bulk density (g/L)	0.56
Specific gravity	1.17
Porosity	51.28
Ash content (%)	1.83
Acid Soluble Matter (%)	1.65
Water Soluble Matter (%)	1.15
Ion Exchange Capacity (meq /g)	0.32
pH_{zpc}	7.07
Surface area (m^2/g)	30.24
Mean Pore diameter (nm)	3.5
Carbon (%)	41.82
Nitrogen (%)	10.78
Hydrogen (%)	5.42
Sulphur (%)	0.52
Surface Acidic groups (m $molg^{-1}$)	
Phenolic	0.72
Carboxylic	1.67
Lactonic	0.21

7.3 SEM and EDAX Analyses

Morphological aspects of raw GGDB are splintery in appearance (fig 7.2), with a lot of small debris and uneven material surface, which appears more uniform and highly porous[3] (fig 7.3) after subjecting to chemical modification. The open pores are appreciably closed due to the sorption of the anionic species indicative of effective chelating property of the material (figs 7.4 – 7.6). Specific sequestration of phosphate, nitrate and sulphate anions is evident from the appearance of new peaks (1- 3 keV) in EDAX spectra corresponding to phosphorous, nitrogen and sulphur atoms (figs 7.8 - 7.10).

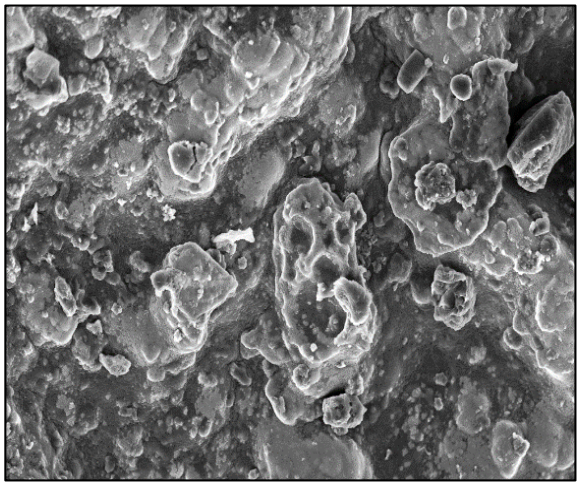

Figure 7.2 Raw GGDB

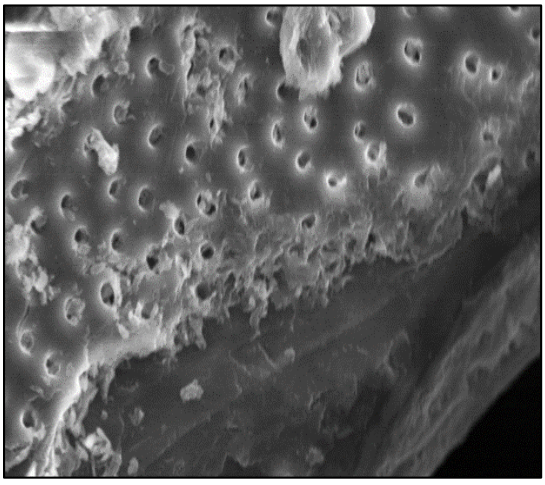

Figure 7.3 Unloaded TGGDB

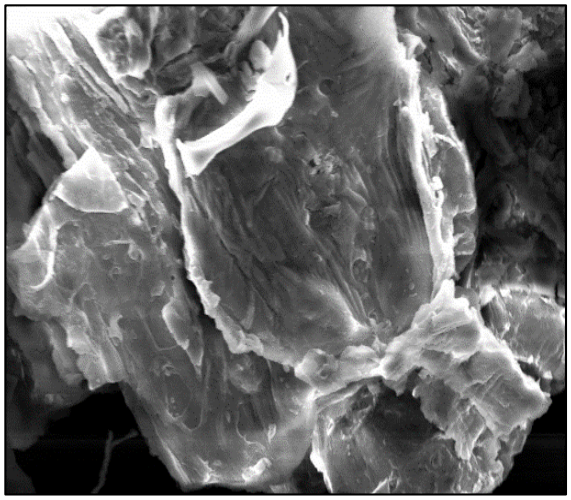

Figure 7.4 PO_4^{3-} loaded TGGDB

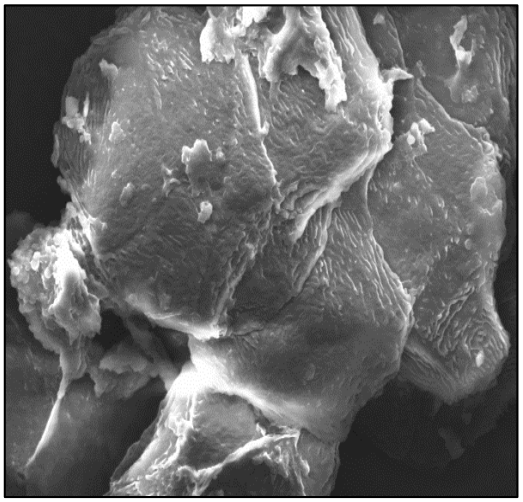

Figure 7.5 NO_3^- - loaded TGGDB

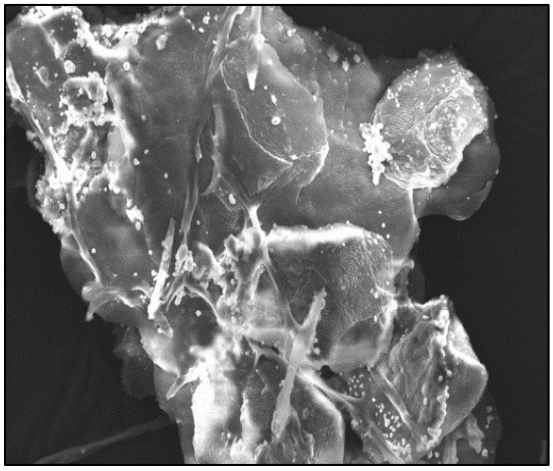

Figure 7.6 SO_4^{2-} - loaded TGGDB

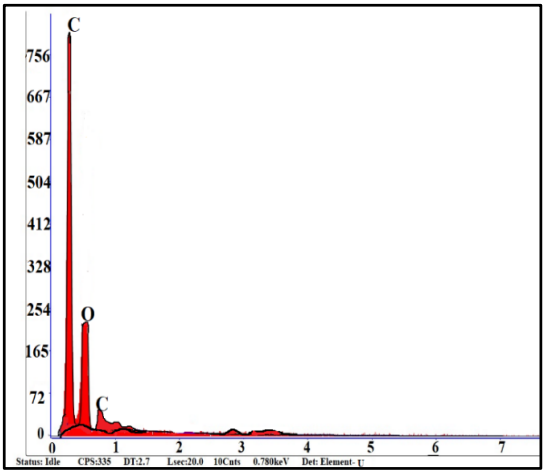

Figure 7.7 Unloaded TGGDB

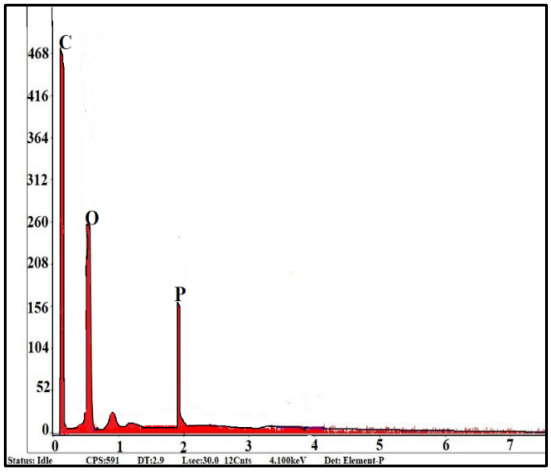

Figure 7.8 PO_4^{3-} loaded TGGDB

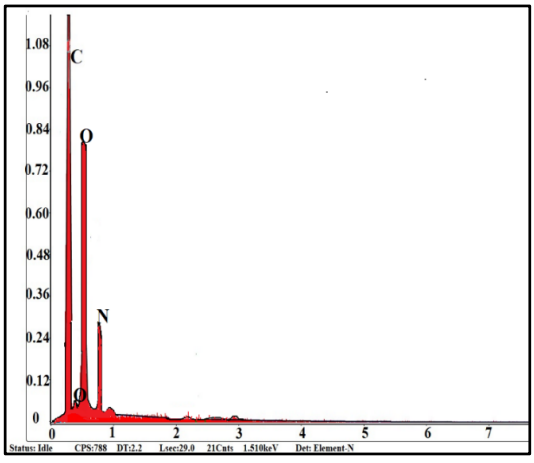

Figure 7.9 NO_3^- loaded TGGDB

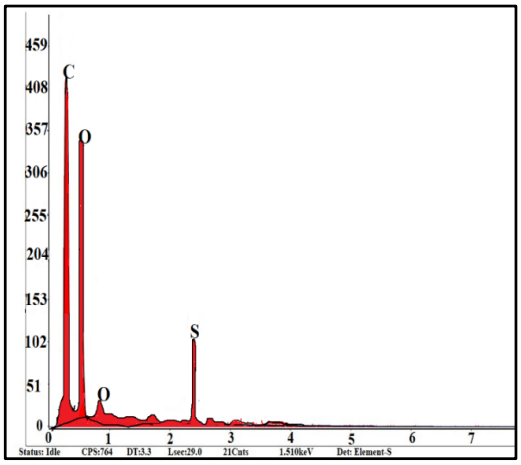

Figure 7.10 SO_4^{2-} loaded TGGDB

7.4 FT- IR Spectral Studies

The functional groups of unloaded and loaded samples are shown in FT-IR spectrum (fig 7.11). All spectral lines show similar characteristics with sorption peaks indicated the complex nature of the sample compositions. A broad band around 3700 cm^{-1}, prominent peaks at 638 cm^{-1}, 999 cm^{-1} correspond to anion binding with the functional groups at the respective O-H, C-H and C-O stretchings[4].

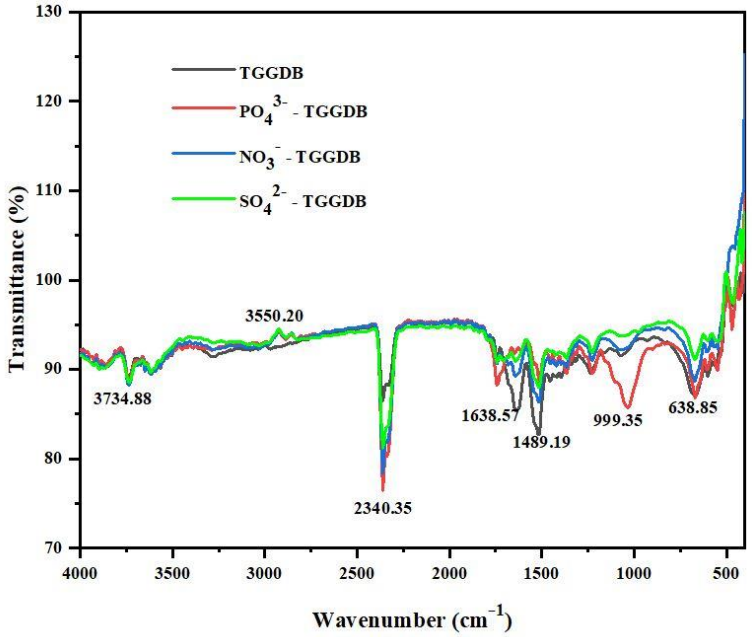

Figure 7.11 FT-IR Spectra

7.5 Batch Equilibration Studies

7.5.1 Impact of TGGDB Particle Size

Anions adsorption of TGGDB for the varying particle sizes as tabulated below, exhibit 0.18 mm size to be appreciable, similar to those observations recorded in the past three chapters.

Table 7.2 Impact of Particle Size

Anions	Amount adsorbed (mg/g)				
	0.18 mm	**0.24 mm**	**0.30 mm**	**0.42 mm**	**0.71mm**
PO_4^{3-}	**42.68**	38.14	33.94	30.12	27.78
NO_3^-	**39.53**	33.32	29.24	26.94	22.93
SO_4^{2-}	**40.97**	35.14	30.69	29.32	26.69

7.5.2 Impact of Initial Concentration and Agitation Time

Varied initial anion concentrations / agitation time intervals (figs 7.12 – 7.14), reveal related conditions of specific concentrations for individual anion with maximal sorption to occurred at an agitation interval at 15 minutes.

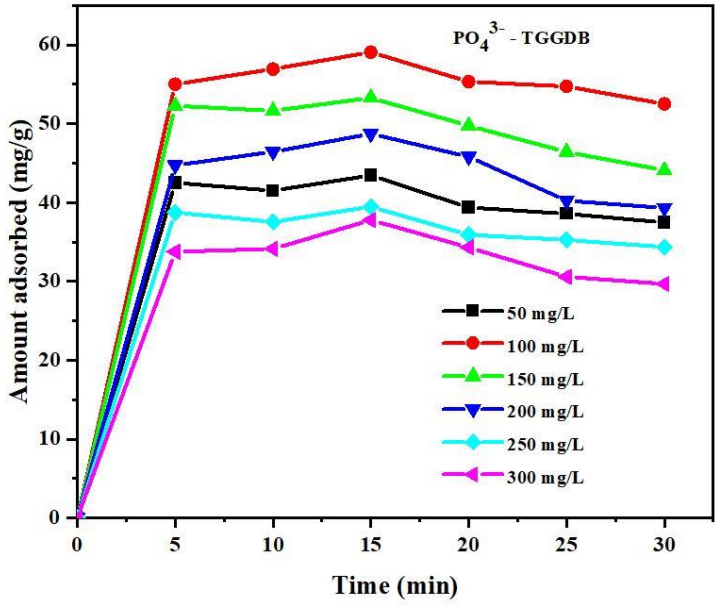

Figure 7.12 Impact of Initial Concentration and Agitation Time: PO_4^{3-}

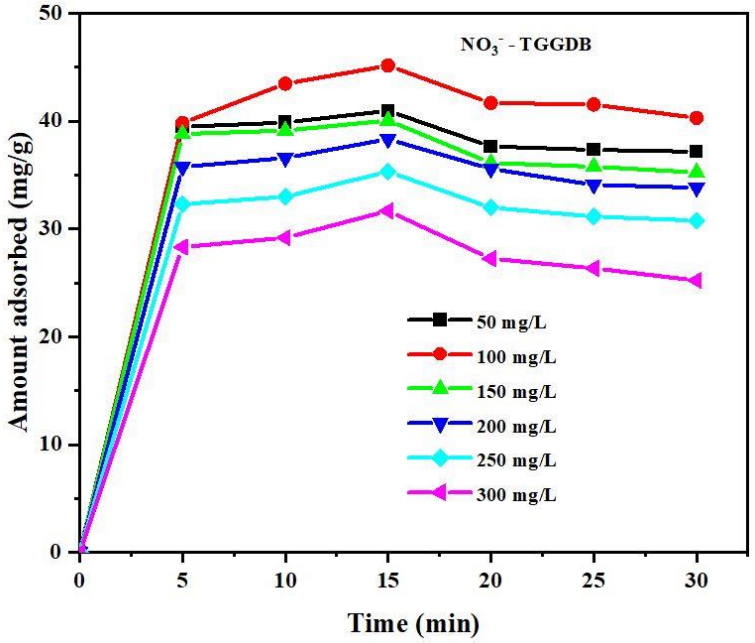

Figure 7.13 Impact of Initial Concentration and Agitation Time: NO_3^-

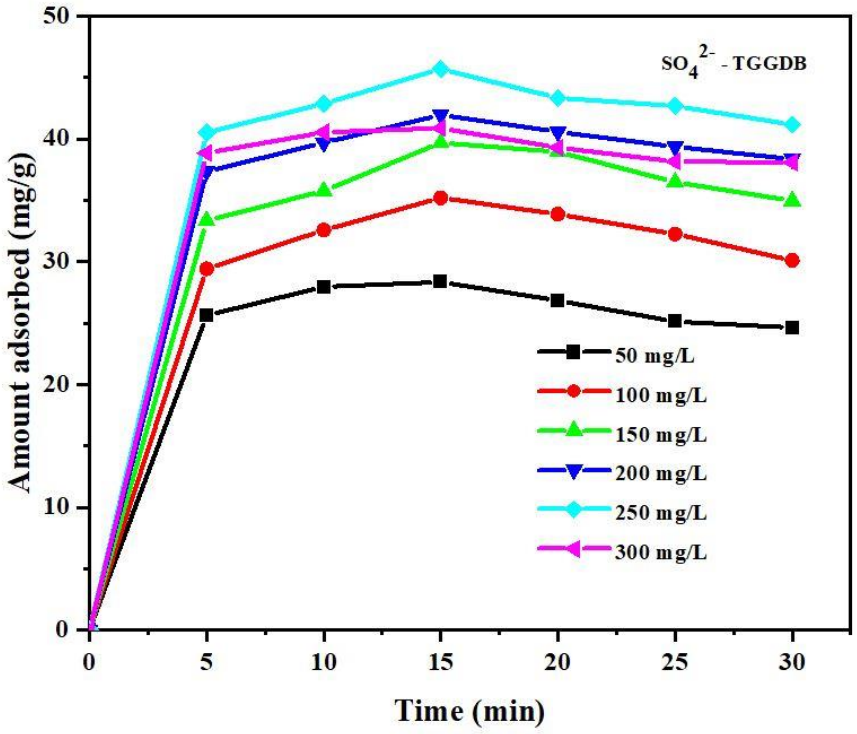

Figure 7.14 Impact of Initial Concentration and Agitation Time: SO_4^{2-}

7.5.3 Impact of TGGDB Dosage

TGGDB masses exhibits extended removal of phosphate/ nitrate and sulphate ions at 200 / 250 mg respectively beyond which there is no appreciable adsorption (Table 7.3). This may be due to conglomeration or active sites saturation at higher dosages [5].

Table 7.3 Impact of Dosage

Anions	Percentage Removal (%)					
	50 mg	**100 mg**	**150 mg**	**200 mg**	**250 mg**	**300 mg**
PO_4^{3-}	76.3	83.8	88.3	**92.5**	90.2	87.4
NO_3^-	73.9	80.5	85.6	**90.8**	86.6	81.9
SO_4^{2-}	75.4	81.4	83.3	89.6	**91.3**	86.3

7.5.4 Impact of pH

Figure 7.15. displays the adsorption efficiency of anions, where a gradual increase is registered to maximum at pH 5, thereafter a long dip in the curves is visible, due to intrusion of similar ionic charges[6].

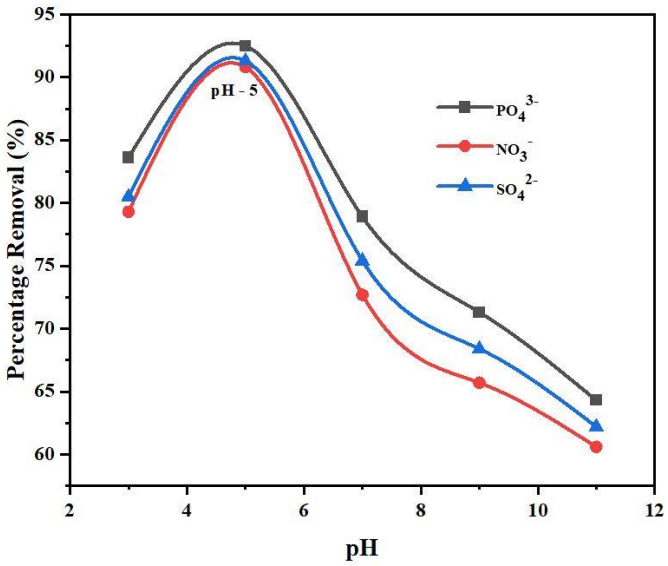

Fig 7.15 Impact of pH

7.5.5 Impact of Ions

Role of interfering ions for TGGDB systems, as mentioned in Table 7.4, imply least inhibition of coions against cationic influence, alike to earlier systems.

Table 7.4 Impact of Ions

Systems	Anion Removal in Absence of ions	Conc. (mg/L)	Percentage Removal (%)			
			Cations		Co ions	
			Mg^{2+}	Na^{+}	Cl^{-}	F^{-}
PO_4^{3-} -TGDDB	92.5	100	**77.8**	80.8	86.2	89.8
		200	76.7	79.6	85.8	88.3
		300	75.3	78.7	84.6	87.4
		400	74.6	77.4	83.5	86.2
		500	73.5	75.9	82.3	85.5
NO_3^{-} - TGDDB	90.8	100	**73.7**	79.6	84.7	87.4
		200	72.4	78.3	83.8	86.6
		300	72.2	77.2	82.6	85.3
		400	71.5	76.9	81.5	84.9
		500	70.9	75.8	80.2	83.7
SO_4^{2-} -TGDDB	91.3	100	**75.8**	80.5	85.7	88.2
		200	74.6	79.3	84.5	87.6
		300	73.3	77.8	83.4	86.4
		400	72.7	76.6	82.2	85.3
		500	71.5	75.4	81.3	84.7

7.5.6 Impact of Temperature

A direct relation between the percentage removal and temperatures is evident from table 7.5, which registers the enrichment of small pores to become wider and accommodate increased number of anions at higher temperature environments.

Table 7.5: Impact of Temperature

Systems	Percentage Removal (%)				
	293 K	**303 K**	**313 K**	**323 K**	**333 K**
PO_4^{3-} TGDDB	88.42	93.92	96.60	96.53	98.70
NO_3^-- TGDDB	85.56	90.84	92.73	95.32	96.58
SO_4^{2-} TGDDB	87.83	91.62	95.73	93.36	97.79

7.5.7 Desorption/ Regeneration Studies

Desorption of chosen anions from TGGDB surface was verified, as mentioned in previous systems. Adsorbed and desorbed amounts were more pronounced for PO_4^{3-} system, against NO_3, SO_4^{2-} systems, in all three cycles, consecutively. This suggests a better regenerating capacity possessed by PO_4^{3-}– TGGDB system.

7.5.8 Statistical Analysis

Statistical data (table 7.6) justifies that anions sorption had occurred at varied operating factors; P values are observed to be less than 0.05 showing similarity in the trends as in the previous chapters.

Table 7.6 Statistical Data

System	Parameter	Descriptive			Pearson Correlation	P	ANOVA	
		Mean	SD	SE			F	F_{crit}
PO_4^{3-} - TGGDB	Particle size	10.14	0.97	0.43	-0.9614	$2.48E^{-05}$	480.09	5.31
	Initial anion concentration	44.14	8.94	3.65	-0.6542	0.0117	11.63	4.96
	Dosage	38.04	3.86	1.57	0.5292	0.0072	12.84	4.96
	pH	35.27	4.04	1.80	-0.7717	0.0003	151.87	5.31
NO_3^-- TGGDB	Particle size	9.73	0.87	0.39	-0.9340	$2.02E^{-05}$	543.43	5.31
	Initial anion concentration	36.99	4.89	1.99	-0.9100	0.0091	13.02	4..96
	Dosage	33.54	3.41	1.39	0.2492	0.0067	13.70	4.96
	pH	31.00	4.66	2.08	-0.8649	0.0010	90.66	5.31
SO_4^{2-} - TGGDB	Particle size	9.34	0.69	0.30	-0.8579	$1.08E^{-05}$	771.65	5.31
	Initial anion concentration	39.61	2.90	1.18	-0.7404	0. 0.0075	12.55	4.96
	Dosage	38.54	5.41	2.20	0.8739	0.0065	12.72	4.96
	pH	33.60	4.01	1.79	-0.8213	0.0004	135.27	5.31

7.6 Adsorption Isotherms

Adsorption behaviour of target anions validated using Langmuir, Freundlich, Temkin and DKR models. Equilibrium Concentrations of the anions and varying sorption capacity of TGGDB are listed in table 7.7, using the above data isothermal plots were constructed and isothermal constants derived from the slopes and intercepts of the respective plots are given in tables 7.8.

Table 7.7 Equilibrium Concentrations- Isothermal Study

System	Anion Conc. (mg/L)	Langmuir		Freundlich		Temkin		DKR	
		C_e	C_e/q_e	log C_e	log q_e	ln C_e	q_e	ε^2*10^{-5}	ln q_e
PO_4^{3-} - TGGDB	50	7.13	1.09	0.85	0.57	1.96	12.47	1.09	2.52
	100	13.58	1.34	1.13	0.61	2.60	21.96	0.32	3.08
	150	19.28	1.47	1.28	0.72	2.95	26.72	0.16	3.39
	200	33.83	1.86	1.73	0.74	3.98	72.65	0.02	4.28
	250	72.31	1.94	1.85	0.82	4.28	87.78	0.01	4.47
	300	98.49	2.01	1.99	0.93	4.58	103.38	0.05	4.63
NO_3^- - TGGDB	50	9.45	1.25	0.97	0.62	2.24	14.12	0.64	2.89
	100	11.15	1.30	1.04	0.54	2.41	23.32	0.46	3.01
	150	25.87	1.47	1.41	0.80	3.25	19.73	0.09	3.39
	200	56.17	1.87	1.82	0.86	4.20	21.86	0.01	4.31
	250	108.61	1.96	1.94	0.96	4.48	22.42	0.05	4.52
	300	133.24	2.07	2.05	0.96	4.72	20.78	0.04	4.76
SO_4^{2-} - TGGDB	50	9.71	1.12	0.98	0.73	2.29	13.28	0.60	2.58
	100	14.23	1.25	1.15	0.79	2.65	21.89	0.29	2.88
	150	25.78	1.45	1.41	0.90	3.24	18.39	0.09	3.34
	200	50.69	1.69	1.66	0.94	3.84	19.59	0.02	3.90
	250	82.57	1.88	1.86	0.95	4.28	20.52	0.01	4.33
	300	130.62	1.98	1.97	0.96	4.53	19.49	0.01	4.50

Table 7.8 Isothermal Constants

System	Langmuir			Freundlich			Temkin			DKR		
	q_m (mg/g)	b	R^2	K_F (mg/g)	1/n	R^2	A_T (L/g)	B_T (J/mol)	R^2	q_s (mg/g)	E (KJ/mol)	R^2
PO_4^{3-} TGGDB	**52.62**	0.06	0.9987	2.56	0.21	0.9149	0.92	69.73	0.8675	37.02	1.36	0.9444
NO_3^- TGGDB	**40.86**	0.02	0.9897	3.12	0.32	0.8232	1.27	67.10	0.8909	26.70	2.55	0.9385
SO_4^{2-} TGGDB	**43.67**	0.04	0.9968	1.70	0.13	0.8895	1.26	70.16	0.9273	30.91	2.41	0.9396

7.6.1 Langmuir Model

Marked q_m values obtained from the linear Langmuir plot (fig 7.16), refers to the notable chelating nature of TGGDB. This observation is supported by the R^2 values, almost unity and R_L values, being less than one[7].

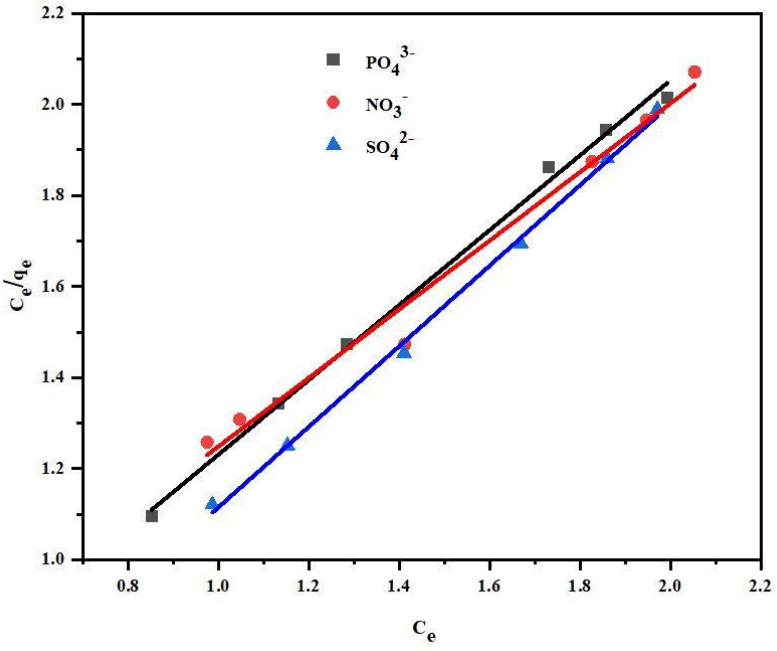

Figure 7.16 Langmuir Plot

7.6.2 Freundlich Model

The applicability of Freundlich model to anions – TGGDB systems is remote as a significant variation is noticed between the qe and K_F values, calculated experimentally and graphically for an optimum concentration.

7.6.3 Temkin Isotherm Model

Lower A_T, higher b_T and deviated correlation coefficient values from unity as evident from table 7.8 corresponds to non-applicability of Temkin model.

7.6.4 Dubinin–Kaganer-Radushkevich (DKR) Model

Similar to previously dealt systems, TGGDB also registered mean free energy values less than 8 KJ/ mol, denoting the sorption mechanism to be physisorption, sufficing the Langmuir isotherm model.[8]

7.6.5 Comparison of Isotherm Models

Calculated q_m values of Langmuir isotherm is observed to be greater than K_F, A_T, q_s constant values of the other studied models. This, implies the system to fit into the former model, thereby favouring monolayer adsorption.

7.7 Adsorption Kinetics

Pseudo first / second order, Elovich and Intra particle diffusions models were employed to examine the experimental data and expressed as follows:

7.7.1 Pseudo First Order/ Pseudo Second Order Models

Experimental data in pertaining to the kinetic plots for the three systems are tabulated (7.9). Constants' values corresponding to the graphical representations given in Table 7.10 are observed to be in lineation with those relevant data mentioned in the previous chapters. Thence, TGGDB systems obey pseudo second order kinetic model[9] (fig 7.17).

Table 7.9 Pseudo Models – Data

Time (min)	PO_4^{3-} - TGGDB			NO_3^-- TGGDB			SO_4^{2-} - TGGDB		
	Log (qe-qt)	qt	t/qt	log (qe-qt)	qt	t/qt	Log (qe-qt)	qt	t/qt
5	1.85	28.66	0.17	1.90	18.73	1.60	1.88	23.54	1.60
10	1.85	27.70	0.36	1.91	17.56	2.30	1.88	22.86	2.30
15	1.86	26.73	0.56	1.91	16.85	2.70	1.89	21.63	2.70
20	1.87	25.54	0.78	1.92	15.72	2.99	1.89	20.58	2.99
25	1.87	24.82	1.01	1.92	14.94	3.21	1.90	19.92	3.21
30	1.88	23.93	1.25	1.93	13.47	3.40	1.91	18.74	3.40

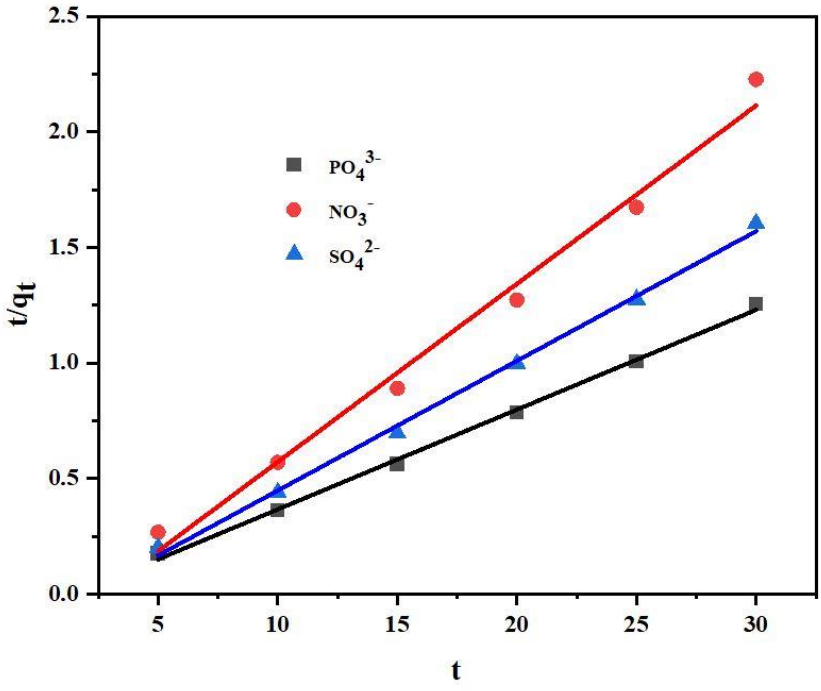

Figure 7.17 Pseudo Second Order Kinetics

Table 7.10 Pseudo First Order/ Pseudo Second Order Parametric Values

Conc. of Anions (mg/L)	q_{exp} (mg/g)	Pseudo First Order				Pseudo Second Order			
		q_{cal} (mg/g)	$K_1 \times 10^{-3}$ (min^{-1})	R^2	SSE	q_{cal} (mg/g)	$K_2 \times 10^{-3}$ (min^{-1})	R^2	SSE
PO_4^{3-} - TGGDB									
50	41.51	31.00	0.0025	0.9437	17.73	46.76	0.0174	0.9987	2.62
100	**56.08**	76.98	0.0122	0.9619	12.96	**53.14**	0.0284	0.9993	1.89
150	51.65	130.16	0.0013	0.9145	39.25	44.64	0.0228	0.9974	3.00
200	44.44	176.21	0.0016	0.9394	65.58	41.64	0.0254	0.9981	0.61
250	37.56	266.42	0.0006	0.9567	115.43	38.79	0.0228	0.9985	0.61
300	32.14	272.41	0.009	0.9186	80.13	36.86	0.0095	0.9989	2.36
NO_3^- - TGGDB									
50	39.86	65.77	0.0089	0.9378	12.95	30.21	0.0156	0.9965	4.82
100	**45.15**	87.31	0.0023	0.9581	21.93	**42.97**	0.0029	0.9987	0.24
150	39.10	157.49	0.0009	0.9514	59.19	36.61	0.0315	0.9983	1.24
200	36.57	180.81	0.0006	0.9552	72.12	33.73	0.0263	0.9978	1.42
250	32.98	263.22	0.0004	0.9214	115.12	30.27	0.0328	0.9959	1.35
300	29.18	282.47	0.0006	0.9548	84.64	33.75	0.0027	0.9972	2.28
SO_4^{2-} - TGGDB									
50	36.34	69.44	0.0331	0.9789	16.55	37.16	0.0170	0.9987	0.41
100	37.19	63.31	0.0020	0.9272	13.06	38.49	0.0287	0.9972	0.60
150	39.67	167.49	0.0016	0.9389	64.04	38.75	0.0198	0.9981	0.46
200	39.93	172.81	0.0011	0.9383	66.28	34.60	0.0183	0.9986	2.66
250	**47.67**	282.22	0.0025	0.9563	18.75	**47.82**	0.0277	0.9993	1.57
300	39.86	285.47	0.0006	0.9199	22.75	32.12	0.0147	0.9982	3.87

7.7.2 Elovich Model

The inverse and direct proportionality of α / β values (Table 7.11) with initial concentrations reveal the inclination in the number of active sites[10], thereby enhancement in the extent of surface coverage by anion species.

Table 7.11 Elovich Constants

Conc. (mg/L)	PO_4^{3-} - TGGDB			NO_3^-- TGGDB			SO_4^{2-} -TGGDB		
	α	β	R^2	α	β	R^2	α	β	R^2
50	25.06	2.51	0.9538	18.31	2.10	0.9419	20.20	2.35	0.9384
100	19.32	2.78	0.9137	12.63	2.39	0.9287	14.04	12.58	0.9253
150	16.46	2.93	0.9106	10.05	2.65	0.9188	11.97	2.88	0.9096
200	13.85	2.95	0.9368	8.51	2.81	0.9096	9.58	2.89	0.9197
250	10.76	3.46	0.9276	6.82	3.13	0.9105	8.19	3.23	0.9341
300	8.36	3.95	0.9379	3.59	3.36	0.9337	5.79	3.70	0.9168

7.7.3 Intraparticle Diffusion Model

Increase in values of boundary layer thickness (C) and Pore diffusion rate (K_{id}) with respect to concentrations are listed in table 7.12, representing external surface adsorption followed by intraparticle diffusion[11].

Table 7.12 Intraparticle Diffusion Constants

Conc. (mg/L)	PO_4^{3-} - TGGDB		NO_3^-- TGGDB		SO_4^{2-} - TGGDB	
	K_{id}	C	K_{id}	C	K_{id}	C
50	1.08	11.92	0.59	1.00	1.01	4.10
100	1.10	15.17	0.91	5.43	1.07	11.61
150	1.28	24.72	0.99	7.39	1.23	14.71
200	1.48	29.92	1.26	9.84	1.34	17.52
250	1.63	34.35	1.49	12.88	1.59	20.77
300	1.88	36.46	1.62	19.56	1.76	26.36

7.7.4 Comparison of Kinetic Models

Pseudo-second-order model provides the best correlation for all the studied systems. Smaller correlation coefficient values with respect to pseudo-first-order/ intraparticle diffusion / Elovich models show their least applicability when compared to pseudo-second-order model.

7.8 Adsorption Dynamics

Thermodynamic variables (ΔG°, Δ*H*°, Δ*S*°) derived from Van't Hoff's plot as represented in previous chapters are noted in table 7.13. Negative ΔG° values (> -1 kJ/mol) confirm the feasible and spontaneous nature of the sorption process[12]. Positive ΔH° and ΔS° values show a greater degree of freedom for the adsorbed species[13], being consistent with the previous data.

Table 7.13 Thermodynamic Constants

Temp. (K)	PO_4^{3-} - TGGDB			NO_3^-- TGGDB			SO_4^{2-} -TGGDB		
	ΔG°x10^{-3} kJ/ mol	ΔH° kJ/ mol	ΔS° kJ/ mol	ΔG°x10^{-3} kJ/ mol	ΔH° kJ/ mol	ΔS° kJ/ mol	ΔG°x10^{-3} kJ/ mol	ΔH° kJ/ mol	ΔS° kJ/ mol
293	0.71	2.94	12.46	-0.87	3.97	16.51	-0.65	3.35	13.68
303	-0.82			-1.03			-0.80		
313	-0.95			-1.15			-0.90		
323	-1.09			-1.32			-1.04		
333	-1.20			-1.56			-1.21		

7.9 References

[1] Vadivel Sivakumar, Manickam Asaithambi and Ponnusamy Sivakumar, Physicochemical and adsorption studies of activated carbon from Agricultural wastes, *Advances in Applied Science and Research,* 3(1) **(2012)** 219-226

[2] Anni Keranen, Tiina Leiviska, Osmo Hormi, Juha Tanskanen, Removal of nitrate by modified pine sawdust: Effects of temperature and co-existing anions, *Journal of Environmental Management,* 147 **(2015)** 46 -54

[3] N.S. Gayathri, N. Muthulakshmi Andal and J. Anuradha, An Investigation Approach on the Sequestration of Divalent Metal Ions Employing Animal Waste, *Oriental Journal of Chemistry*, 33 **(2017)** 1406 - 1413

[4] Laleh Divband Hafshejani a, Abdolrahim Hooshmanda, Abd Ali Naseri a, Amir Soltani Mohammadi a, Fariborz Abbasi b, Amit Bhatnagar, Removal of nitrate from aqueous solution by modified sugarcane bagasse biochar, *Ecological Engineering,* 95 **(2016)** 101- 111

[5] Mahmoud El Ouardi, Samir Qourzal, Said Alahiane, Ali Assabbane, Jamaa Douch, Effective Removal of Nitrates Ions from Aqueous Solution Using New Clay as Potential Low-Cost Adsorbent, *Journal of Encapsulation and Adsorption Sciences*, 5 **(2015)** 178-190

[6] Paula Szymczyk, Urszula Filipkowska, Tomasz Jóźwiak, Małgorzata Kuczajowska-Zadrożna, Phosphate Removal from Aqueous Solutions by Chitin and Chitosan in Flakes, *Progress on Chemistry and Application of Chitin and its Derivatives*, XXI **(2016)** 192 - 202

[7] Artis Robalds, Liga Dreijalte, Oskars Bikovens and Maris Klavins, A Novel Peat-based Biosorbent for the Removal of Phosphate from Synthetic and Real Wastewater and Possible Utilization of Spent Sorbent in Land Application, *Desalination and Water Treatment,* 57 **(2016)** 13285–13294

[8] Vishal R. Parate, Mohammed.I.Talib, Study of Metal Adsorbent Prepared from Tur Dal (*Cajanus cajan*) Husk: A Value Addition to Agro-waste, IOSR Journal of Environmental Science, Toxicology and Food Technology, 9(3) **(2014)** 43- 54

[9] R.Apiratikul, T.F.Marhaba, S.Wattanachira, P.Pavasant, 'Biosorption of binary mixtures of heavy metals by green macro alga Caulerpa lentillifera, *Journal of Science and Technology*, 26 **(2004)** 199–207

[10] Bulut Yasemin, Tez Zeki, Removal of heavy metals from aqueous solution by sawdust adsorption, *Journal of Environmental Science*, 19 **(2007)** 160-166

[11] Afkhami, A., Madrakian, T., Karimi, Z., The effect of acid treatment of carbon cloth on the adsorption of nitrite and nitrate ions, *Journal of Hazardous Material* 144 **(2007)** 427-431

[12] Linan Liu, Lihua Wang, Liming Yin, Wenhong Song, Jinghnu Yu and Ye Lin, Effects of Different Solvents on the Surface Acidic Oxygen – containing Functional Groups on *Xanthoceras sorbifolia* Shell, *Bio Resources*, 9(2) **(2014)** 2248- 2258

[13] Mahmoud Mazarji, Behnoush Aminzadeh, Majid Baghdadi, Amit Bhatnagar, Removal of nitrate from aqueous solution using modified granular activated carbon, *Journal of Molecular Liquids*, 17 **(2017)** 1 – 48.